MAML1, a human homologue of *Drosophila* Mastermind, is a transcriptional co-activator for NOTCH receptors

Lizi Wu[1], Jon C. Aster[2], Stephen C. Blacklow[2], Robert Lake[3], Spyros Artavanis-Tsakonas[3] & James D. Griffin[1]

Notch receptors are involved in cell-fate determination in organisms as diverse as flies, frogs and humans[1]. In *Drosophila melanogaster*, loss-of-function mutations of *Notch* produce a 'neurogenic' phenotype in which cells destined to become epidermis switch fate and differentiate to neural cells. Upon ligand activation, the intracellular domain of Notch (ICN) translocates to the nucleus[2], and interacts directly with the DNA-binding protein Suppressor of hairless (Su(H)) in flies, or recombination signal binding protein Jκ (RBP-Jκ) in mammals[3], to activate gene transcription[4]. But the precise mechanisms of Notch-induced gene expression are not completely understood. The gene *mastermind* has been identified in multiple genetic screens for modifiers of *Notch* mutations in *Drosophila*[5–8]. Here we clone *MAML1*, a human homologue of the *Drosophila* gene *Mastermind*, and show that it encodes a protein of 130 kD localizing to nuclear bodies. MAML1 binds to the ankyrin repeat domain of all four mammalian NOTCH receptors, forms a DNA-binding complex with ICN and RBP-Jκ, and amplifies NOTCH-induced transcription of *HES1*. These studies provide a molecular mechanism to explain the genetic links between *mastermind* and *Notch* in *Drosophila* and indicate that MAML1 functions as a transcriptional co-activator for NOTCH signalling.

We isolated *MAML1* (for mastermind-like-1), a human gene encoding a protein related to *Drosophila* Mastermind, particularly in the amino-terminal basic domain (35% amino acid identity and 51% similarity; Fig. 1*a*). Northern-blot analysis disclosed a single, 6-kb transcript in all tissues examined (Fig. 1*b*), and an additional 1-kb transcript in placenta.

We used a series of N-terminal truncations of MAML1 fused to green fluorescence protein (GFP) to examine subcellular localization. MAML1–GFP localized to nuclear dots (Fig. 2*a*). Deletion of the N-terminal 123 amino acids resulted in loss of punctate staining, but not nuclear localization, in COS7, HeLa and U2OS cells. A further truncation containing the putative nuclear localization signal resulted in both cytoplasmic and nuclear staining. An anti-MAML1 monoclonal antibody (8E6B10) confirmed punctate nuclear staining, indicating that localization to nuclear dots is not an artefact of fusion to GFP or overexpression (data not shown). In most cells, MAML1 colocalized with promyelocytic leukaemia (PML) protein (Fig. 2*b*).

We next looked for colocalization of MAML1 with ICN and RBP-Jκ. ICN1–GFP localized to the nucleus in a diffuse pattern (Fig. 2*c*). Co-expression of MAML1 altered ICN1–GFP distribution to the punctate pattern of MAML1. MAML1–GFP colocalized with ICN1 in these dots (Fig. 2*d*). RBP-Jκ also relocated into nuclear dots with MAML1 when ICN1 was present (Fig. 2*e*). Like MAML1, Mastermind also colocalized with ICN1 in nuclear dots in 293T cells (data not shown), suggesting conservation of function between *Drosophila* Mastermind and human MAML1, despite their limited sequence similarity.

These results indicate that MAML1, ICN1 and RBP-Jκ might form a complex. In support of this, MAML1 co-immunoprecipitated with ICN1, and this was enhanced by RBP-Jκ (Fig. 3*a*). MAML1 co-immunoprecipitated with RBP-Jκ, but only in the presence of ICN1. MAML1 similarly co-immunoprecipitated

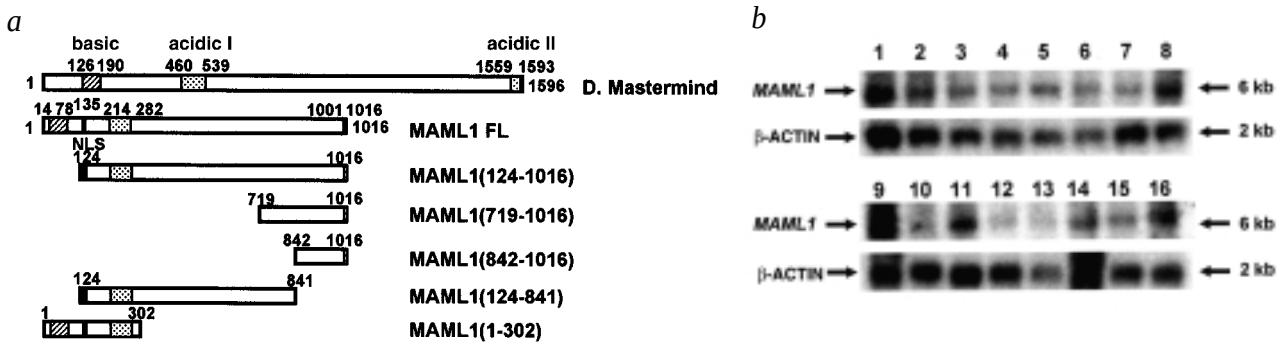

Fig. 1 MAML1 structure and expression. ***a***, Comparison of domain organization between MAML1 and *Drosophila* Mastermind, and schematic of full length (FL) and truncated mutant MAML1 proteins. Alignment of amino acid sequence of MAML1 and *Drosophila* Mastermind, generated by the Pileup program in GCG (Wisconsin Package Version 9.0) and refined by Boxshade 3.21 (http://www.ch.embnet.org/software/box_form.html; see Fig. A, http://genetics.nature.com/supplementary_info/). The overall amino-acid identity and similarity was 24% and 27%, respectively. *MAML1* was cloned from a HeLa cDNA library using a yeast two-hybrid system with the E6 oncoprotein of human papillomavirus as a bait. A possible nuclear localization signal (NLS), PGHKKTR, was identified at aa 135–141. MAML1 has a predicted molecular weight of 108 kD. The apparent molecular weight on reducing SDS–PAGE of endogenous and transfected MAML1 proteins is ~130 kD. ***b***, Northern-blot analysis of *MAML1* expression in human tissues. Lane 1, spleen; lane 2, thymus; lane 3, prostate; lane 4, testis; lane 5, ovary; lane 6, small intestine; lane 7, colon; lane 8, peripheral blood leukocyte; lane 9, heart; lane 10, brain; lane 11, placenta; lane 12, lung; lane 13, liver; lane 14, skeletal muscle; lane 15, kidney; lane 16, pancreas. A single 6-kb transcript of *MAML1* was present in these tissues with an additional 1-kb transcript in placenta (not shown). The hybridization with β-actin served as the RNA-loading controls.

[1]*Department of Adult Oncology, Dana-Farber Cancer Institute and Departments of Medicine, Brigham and Women's Hospital and Harvard Medical School;* [2]*Department of Pathology, Brigham and Women's Hospital, and Department of Pathology, Harvard Medical School;* [3]*Cancer Center, Massachusetts General Hospital, and Department of Cell Biology, Harvard Medical School, Boston, Massachusetts, USA. Correspondence should be addressed to J.D.G. (e-mail: james_griffin@dfci.harvard.edu).*

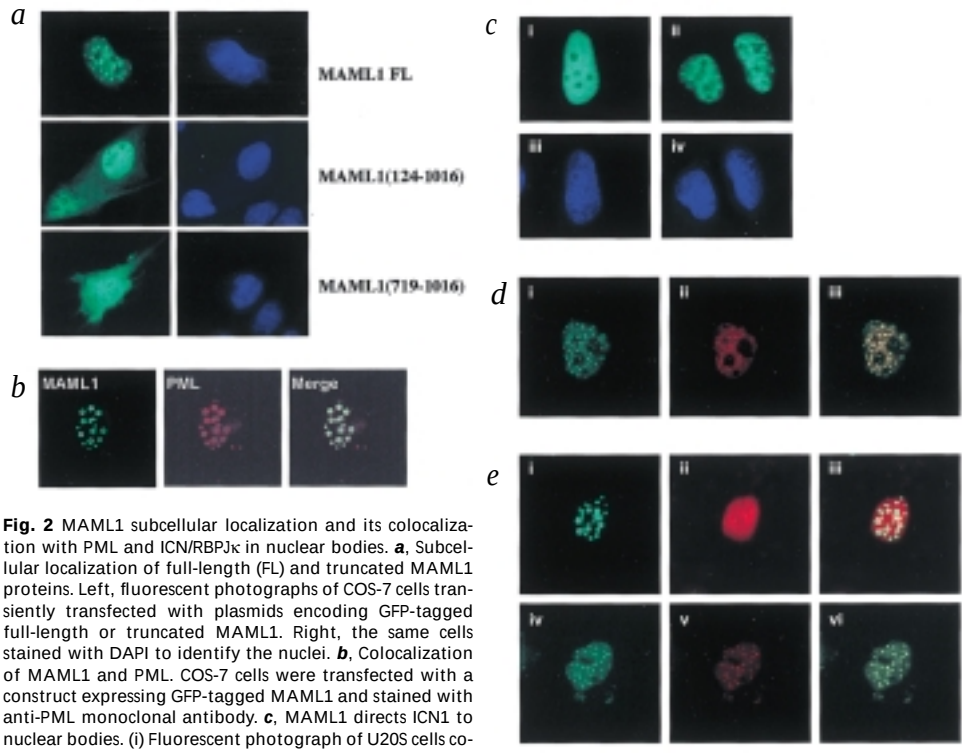

Fig. 2 MAML1 subcellular localization and its colocalization with PML and ICN/RBPJκ in nuclear bodies. ***a***, Subcellular localization of full-length (FL) and truncated MAML1 proteins. Left, fluorescent photographs of COS-7 cells transiently transfected with plasmids encoding GFP-tagged full-length or truncated MAML1. Right, the same cells stained with DAPI to identify the nuclei. ***b***, Colocalization of MAML1 and PML. COS-7 cells were transfected with a construct expressing GFP-tagged MAML1 and stained with anti-PML monoclonal antibody. ***c***, MAML1 directs ICN1 to nuclear bodies. (i) Fluorescent photograph of U2OS cells co-transfected with a construct expressing GFP-tagged ICN1 and a pFLAG-CMV-2 empty vector. (ii) U2OS cells co-transfected with constructs expressing GFP-tagged ICN1 (visualized here) and FLAG-tagged MAML1 (not stained in this panel). (iii, iv) DAPI staining of the same cells to identify the nuclei. ***d***, Colocalization of MAML1 and ICN1. COS-7 cells were co-transfected with constructs expressing GFP-tagged MAML1 and HA-tagged ICN1. (i) GFP-tagged MAML1. (ii) ICN-1 detected by immunofluorescent staining with anti-HA. (iii) MAML1 and ICN-1 merged. ***e***, ICN1-dependent MAML1 and RBP-Jκ colocalization. COS-7 cells were co-transfected with constructs expressing GFP-tagged MAML1 and Myc-tagged RBP-Jκ in the absence (i–iii) and the presence (iv–vi) of ICN1. (i,iv) GFP-tagged MAML1; (ii, v) RBP-Jκ detected by immunofluorescent staining with anti-Myc; (iii,vi) merged figures. The size of the dots in individual cells was not related to transfection of any construct.

with ICN2, ICN3 and ICN4 (Fig. 3*b*). Co-immunoprecipitation required the N-terminal 123 amino acids of MAML1, and an N-terminal fragment of 302 amino acids from MAML1 was sufficient to form a complex with both ICN1 and RBP-Jκ (Fig. 3*c*).

We carried out *in vitro* binding studies to determine if MAML1 bound directly to ICN1–4. GST–MAML1 beads bound substantially more ICN1–4 than control GST beads (Fig. 4*a*). Binding of ICN1 to MAML1–GST was enhanced in the presence of RBP-Jκ, and required the presence of the ICN1 ankyrin repeats. The ability of MAML1 to associate with ICN1 and RBP-Jκ bound to DNA was evaluated with an electrophoretic mobility shift assay (Fig. 4*b*). A single complex was identified when partially purified RBP-Jκ was added to a labelled oligonucleotide containing RBP-Jκ binding sites[4]. The further addition of both the RAM-ankyrin repeat region (RAM-ANK) of NOTCH1 (residues 1,760–2,126) and MAML1(1–300) shifted the RBP-Jκ/DNA complex, whereas addition of either RAM-ANK or MAML1 alone had no effect. The ANK region without the RAM domain (residues 1,872–2,126) failed to shift the RBP-Jκ/DNA complex, even in the presence of MAML1. The higher molecular weight complex formed by RBP-Jκ, RAM-ANK and MAML1 was supershifted by an antibody specific for MAML1, confirming the presence of MAML1 in the complex. Overall, these studies are consistent with MAML1 acting to stabilize the association of ICN and RBP-Jκ through the formation of a ternary complex.

We investigated the functional importance of MAML1/ICN interaction by examining NOTCH-induced activation of a *HES1* promoter construct[4]. *HES1* promoter activation induced by Jagged2 was increased 5–10-fold by co-transfection with MAML1 (Fig. 5*a*). MAML1 increased *HES1* activity 2–3-fold in the absence of Jagged2. Similarly, co-expression of MAML1 with submaximal amounts of ICN1 led to a potentiation of reporter activity (Fig. 5*b*). A *HES1* reporter lacking RBP-Jκ sites[4] was not activated. MAML1 also increased *HES1* reporter activity induced by ICN2, ICN3 and ICN4 by more than tenfold (Fig. 5*c*). These results suggested that MAML1 might function as a transcriptional co-activator for NOTCH receptors. A transcriptional activation domain (TAD) was identified in the carboxy terminus of MAML1 by fusing full-length or truncated MAML1 directly to the DNA-binding domain of GAL4 (Fig. 5*d*).

Previous studies of ICN1 have identified the ankyrin repeats and the C-terminal region of ICN1 as possible binding sites for co-activators[9,10]. When overexpressed with MAML1, the ANK domain of ICN1 was sufficient to activate the *HES1* reporter (data not shown). Thus, the binding of MAML1 may explain in part previous studies showing a critical role for this region[10,11].

Our experiments suggest a model in which the N-terminal basic domain of MAML1 forms a complex with ICN and RBP-Jκ, and activates transcription of NOTCH-dependent genes through its C-terminal TAD. We tested this model by determining if truncation mutants of MAML1 might function as dominant-negative inhibitors of NOTCH. Both MAML1(1–302) (defective in transactivation) and MAML1(124–1,016) (defective in Notch binding) reduced activation of *HES1* by Jagged2 in U2OS cells (Fig. 6*a*,*b*) and NIH3T3 cells (data not shown). The dominant-negative effects of MAML1(1–302) on transcription are consistent with previous studies showing that C-terminal truncations of *Drosophila* Mastermind disrupt Notch pathway function in eye and wing development[12].

Previous studies on the mechanism of Notch-induced gene transcription have focused on two potential mechanisms: the displacement of co-repressors from RBP-Jκ by ICN and the possible recruitment of co-activators. Several co-repressors have been identified, including CIR (ref. 13), SMRT (ref. 14) and KyoT2 (ref. 15). SKIP has also been shown to link RBP-Jκ to co-repressor molecules[16].

We have identified a homologue of *Drosophila* Mastermind that binds to the ankyrin repeats of ICN, forms a DNA-binding complex with ICN and RBP-Jκ, and potentiates NOTCH-induced transcription from a *HES1* promoter. MAML1 contains a C-terminal TAD, providing a mechanism for the observed effects on transcription. The ankyrin repeats have other critical functions, including participating in the interaction of ICN with Su(H), and binding Deltex, a positive regulator of Notch signalling that can displace Su(H) (refs 17,18). Recently, LAG-3 was found to bind to the ankyrin repeats of

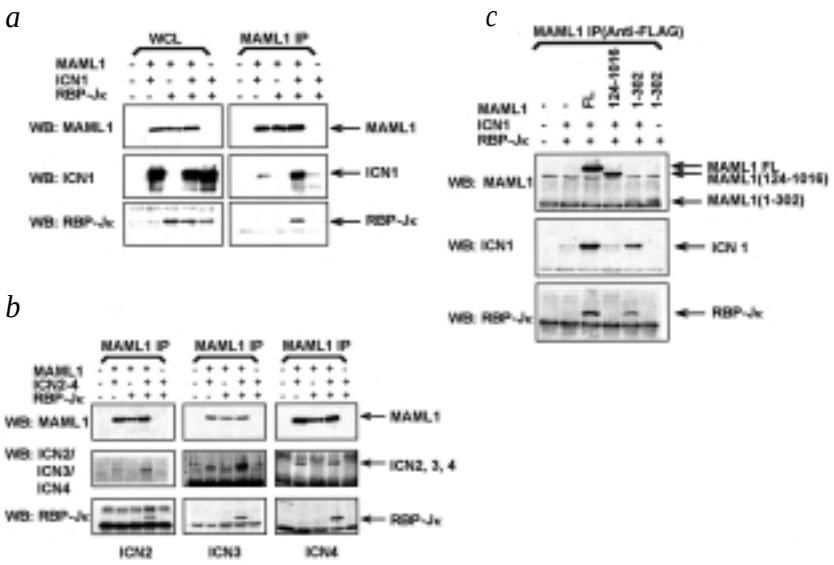

Fig. 3 Detection of a ternary complex of MAML1, ICN and RBP-Jκ *in vivo*. ***a***, MAML1, ICN1 and RBP-Jκ co-immunoprecipitate. COS-7 cells were co-transfected with different combinations of three constructs encoding FLAG-tagged MAML1, HA-tagged ICN1 and Myc-tagged RBP-Jκ. In this and subsequent co-transfection experiments, the total amount of plasmids for each transfection was equalized by supplementing with empty vectors. At 44 h post-transfection, cell lysates were analysed either directly (50 μg protein/lane) or following immunoprecipitation (500 μg lysate protein immunoprecipitated with anti-FLAG antibody M2 from Sigma) on western blots probed with anti-FLAG, anti-HA or anti-Myc. ***b***, MAML1, ICN2-4 and RBP-Jκ form a ternary complex *in vivo*. COS-7 cells were co-transfected with different combinations of three constructs encoding FLAG-tagged MAML1, ICN2 (or HA-ICN3, or ICN4) and Myc-tagged RBP-Jκ and immunoprecipitated as above. Immunoprecipitates were analysed on western blots probed with anti-FLAG, anti-ICN2, anti-HA, anti-ICN4 goat antibody or anti-Myc. ***c***, The MAML1 N-terminal 123 aa, which contain the basic domain, are required for ICN binding. COS-7 cells were co-transfected with three constructs encoding HA-tagged ICN1 and Myc-tagged RBP-Jκ, along with either FLAG-tagged MAML1 FL, MAML1(124–1,016), or MAML1(1–302), and analysed by immunoprecipitation and immunoblotting.

GLP-1 and LIN-12, and the *Caenorhabditis elegans* Notch receptors, and to contain a transcriptional activation domain[19]. Despite the functional similarities between MAML1 and LAG-3, however, there is minimal sequence similarity, and it is not clear if they are in the same gene family.

The role of nuclear bodies in NOTCH signalling warrants further investigation, as MAML1 causes the redistribution of ICN and RBP-Jκ to these nuclear structures. PML bodies have been linked to transcriptional regulation, and both transcription factors and transcriptional co-activators have been detected in these organelles[20,21]; however, the functions of PML bodies and other nuclear dots remain largely unknown.

Overall, our results suggest a role for MAML1 in signalling of all four mammalian NOTCH receptors. Moreover, these studies provide a potential mechanism to explain some of the previously described genetic interactions of *Drosophila* Mastermind with the Notch pathway[22,23].

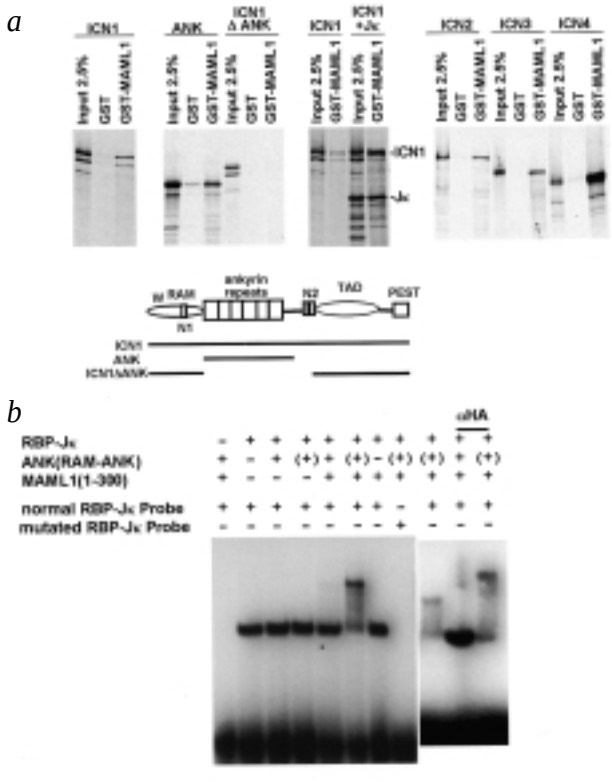

Fig. 4 MAML1 binds directly to the anykyrin repeats of NOTCH. ***a***, Detection of a MAML1, ICN and RBP-Jκ ternary complex *in vitro*. ^{35}S-labelled polypeptides were generated by *in vitro* transcription/translation with the TNT reticulocyte lysate system, and binding of ^{35}S-labelled proteins to GST or GST–MAML1 glutathione beads was measured. For comparison, 2.5% of the *in vitro* translation product is shown with precipitation on GST beads. The structures of the ICN1 polypeptides used here are shown in the diagram. ***b***, Binding of MAML1 to ICN and RBP-Jκ in a DNA-binding complex by electrophoretic mobility shift assays. The indicated combinations of partially purified RBP-Jκ, purified ANK or RAM-ANK fragments of NOTCH1, and MAML1 (residues 1–300 with an HA tag) were added to ^{32}P-labelled oligonucleotides containing a normal or mutated RBP-Jκ-binding site[28] before gel electrophoresis (left). In a separate experiment, anti-HA antibody was added to supershift DNA binding complexes containing MAML1 (right). +, –, Presence or absence of the individual components listed on the left, respectively. (+), The addition of RAM-ANK instead of ANK.

Methods

Plasmids. We obtained the bait construct used for yeast two-hybrid screening (pDBLeu-16E6) by PCR-amplifying the full-length E6 sequence derived from HPV type 16 E6 (cDNA was provided by P. Howley). We then cloned this cDNA into the *Sal*I-*Not*I sites of pDBLeu (Gibco-BRL) in-frame with a sequence encoding the DNA-binding domain (DB) of GAL4. We cloned MAML1 full-length (FL), MAML1(124–1016), MAML1(719–1016), MAML1(842–1016) MAML1(124–841) and MAML1(1–302) sequences as *Sal*I-*Not*I fragments into pFLAG-CMV-2 (Sigma), pEGFP-C3 (Clontech), pGEX-2TK (Stratagene) and pBIND (Promega) vectors. MSCV-GFP (ref. 24) is a derivative of MSCV (ref. 25). cDNAs encoding ICN1, ICNΔANK (ref. 26), ICN2 (ref. 18) and Myc-epitope tagged RBP-Jκ (ref. 27) have been described. We fused a sequence encoding three copies of the HA epitope with the human ICN1 cDNA after replacement of the 3′ stop codon with an in-frame 3′ *Xho*I site created using PCR. A mouse ICN3 cDNA was obtained from U. Lendahl. We amplified a human cDNA encoding ICN4 by PCR from a human umbilical vein cDNA library, and then sequenced and ligated this ICN4 cDNA into pcDNA3. *HES1*-luc contains the –194 to +160 promoter fragment of *HES1* cloned upstream of the firefly luciferase gene in the pGL2-basic vector[4]. *HES1*(ΔAB)-luc, derived from *HES1*-luc, has a deletion removing the two RBP-Jκ-binding sites[4]. To normalize firefly luciferase activities for transfection efficiency, we co-transfected cells with either pCMX-lacZ or pRL-TK

(Promega), which encode β-galactosidase and *Renilla* luciferase, respectively. pSG5-luc (Promega) is a firefly luciferase reporter plasmid that contains five copies of GAL4-binding site upstream of a minimal TATA box.

Antibodies. We purchased the following antibodies from commercial sources: mouse anti-Flag antibody (clone M2, Sigma); mouse anti-HA monoclonal antibody (clone HA.11, Babco); mouse anti-PML monoclonal antibody (PG-M3), goat anti-NOTCH4, goat anti-mouse IgG and goat anti-rat IgG antibodies (Santa Cruz Biotechnology); horseradish peroxidase (HRP)-coupled goat anti-mouse and goat anti-rabbit IgG antibodies (Amersham); and Rhodamine Red-X-conjugated $F(ab')_2$ fragment goat anti-mouse antibody (Jackson ImunoResearch Laboratories). Anti-Myc (clone 9E10) monoclonal antibody was obtained from J. Parvin.

Cell culture and transient transfection. We cultured human U2OS osteosarcoma cells in Dulbecco's modified Eagle's medium (DMEM) containing 10% Fetalclone I serum (HyClone Laboratories), and COS7 cells in RPMI 1640 medium supplemented with 10% fetal calf serum (FCS). NIH 3T3 cells transduced by pBABE retrovirus encoding Jagged2, or empty pBABE retrovirus, were maintained in DMEM medium containing 10% FCS and puromycin (1 μg/ml). We carried out transfections using Superfect transfection reagent (Qiagen) according to the manufacturer's instructions.

Yeast two-hybrid screening. Yeast two-hybrid screening (Proquest, Gibco-BRL) was performed on a HeLa cell expression library fused to the Gal4 activation domain (AD) in the *Sal*I-*Not*I sites of the pPC86 vector according to the manufacturer's instructions. We screened ~3.4×10^6 transformants and obtained 20 positive clones. Plasmids containing the prey sequences were rescued and checked by retransformation with the bait into yeast. Finally, we sequenced the prey inserts obtained from the positive clones. In this screening, we obtained three novel proteins in addition to the known E6 binding proteins (E6AP and E6TP1). One of these, MAML1, was defined by four overlapping cDNAs. We sequenced the longest *MAML1* cDNA (5.1 kb), and found that it was derived from a previously sequenced full-length cDNA (5.7 kb) generated randomly from a KG-1 library, KIAA0200, except MAML1 has Asn instead of Ser at position 1,007. We obtained a full-length *MAML1* cDNA by ligating a 709-bp *Sma*I-*Bcl*I fragment of KIAA0200 (obtained from Kazuza DNA Research Institute, Japan) to the appropriate site in the *MAML1* E12 cDNA.

Northern-blot analysis. Filter-immobilized polyadenylated RNAs from multiple human tissue blots (Clontech) were hybridized with ^{32}P-labelled *MAML1* (nt 369–2,160 of the *MAML1* ORF) and β-actin cDNA probes according to the manufacturer's instructions.

Immunofluorescence staining. We fixed cells grown on coverslips in 4% paraformaldehyde in PBS for 20 min. After permeabilization in 0.1% NP-40 in PBS for 15 min, non-specific binding sites were blocked with 5% non-immune goat serum in PBS for 15 min. We then incubated cells for 60 min with PBS/0.1% NP-40/5% goat serum containing primary antibody, washed cells extensively with PBS/0.1% NP-40, and then incubated cells for 60 min with secondary antibody in PBS/0.1% NP-40/5% goat serum. After washing extensively, coverslips were mounted in Gel/mount medium (Biomeda) and photographed with an Olympus microscope and a SPOT camera (Diagnostic Instrument). Composite images were generated by SPOT software V2.2 (Diagnostic Instruments).

Western-blot analysis and immunoprecipitation. We seeded COS7 cells on 100-mm plates at 5×10^5 cells per plate one day before transfection, and transiently transfected cells with various combinations of expression plasmids. We kept the total amounts of plasmids constant by adding appropriate amounts of empty vectors without inserts. At 44–48-h post-transfection, we washed cells with ice-cold PBS and lysed cells *in situ* with a solution containing Tris (20 mM, pH 8.0), NaCl (150 mM), 1% NP-40 (w/v), 10% glycerol

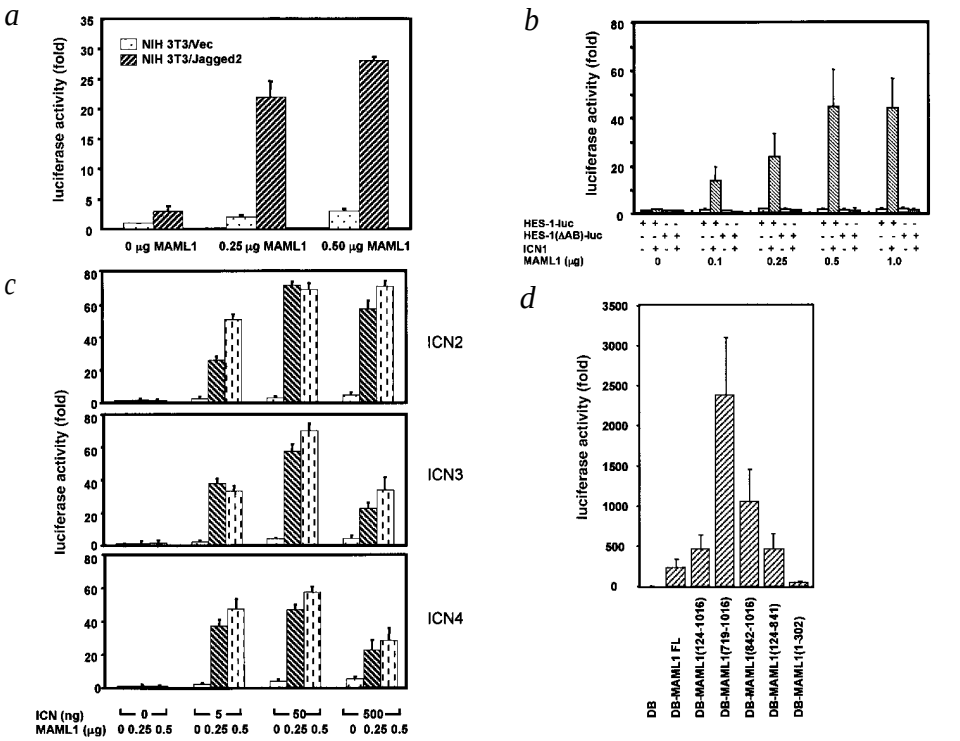

Fig. 5 MAML1 cooperates with NOTCH to activate the *HES1* promoter. ***a***, MAML1 augments ligand-induced NOTCH activation. U20S cells were transfected with a β-galactosidase control plasmid (0.5 μg), *HES1*-luc (0.5 μg) and increasing amounts of pFLAG-CMV-2 plasmid encoding *MAML1*. Twenty hours post-transfection, 1×10^5 NIH 3T3 cells expressing Jagged2 or NIH 3T3 cells infected with empty pBABE virus were added to each well. Except as noted, in all HES1 transfection assays, cell extracts were prepared 44 h post-transfection. *HES1* reporter luciferase activity, corrected for β-galactosidase activity, is expressed as fold activation relative to cells not expressing MAML1 that were co-cultured with control NIH 3T3 cells. Error bars indicate standard deviation of three independent experiments. ***b***, Activation of *HES1* promoter by MAML1 requires ICN1 and RBP-Jκ binding sites. U20S cells were transfected with β-galactosidase control reporter construct, luciferase reporter construct, *HES1*-luc or *HES1*(ΔAB)-luc, and increasing amounts of pFLAG-CMV plasmid encoding MAML1, in the absence or presence of MSCV-ICN1 plasmid. Luciferase activity, corrected for β-galactosidase activity, was expressed as fold activation relative to cells with no expression of MAM and ICN1. When tested with the ICN1 driven by strong promoter (a pcDNA3 vector encoding ICN1), the enhancing effects of MAML1 on *HES1* transcription were prominent at low levels of ICN1 expression, but decreased with higher, possibly non-physiologic, levels of ICN1 (levels where activation of the *HES1* promoter by ICN1 alone was higher than what could be achieved with Jagged2 signalling; data not shown). ***c***, Cooperative activation of the HES1 promoter by MAML1 and ICN2, ICN3 and ICN4. U20S cells were transfected as above with increasing amounts of pFLAG-CMV-2 plasmid encoding MAML1 in the presence of pcDNA3 plasmids encoding human ICN2, mouse ICN3 or human ICN4. ***d***, MAML1 is a transcriptional co-activator. U20S cells were transfected with a firefly luciferase construct (1 μg) containing four GAL4 binding sites (pG5luc) and pBIND plasmid (1 μg) encoding either the GAL4 DNA binding domain (DB), DB fused to full-length MAML1, or DB fused to the indicated MAML1 deletion mutants. Firefly luciferase activity, normalized to *Renilla* luciferase expressed from the pBIND plasmid, was expressed as fold activation relative to the background level of firefly luciferase expression in the presence of an empty pBIND vector. No transcriptional activation activity was observed in the absence of the GAL4 DNA-binding domain (data not shown).

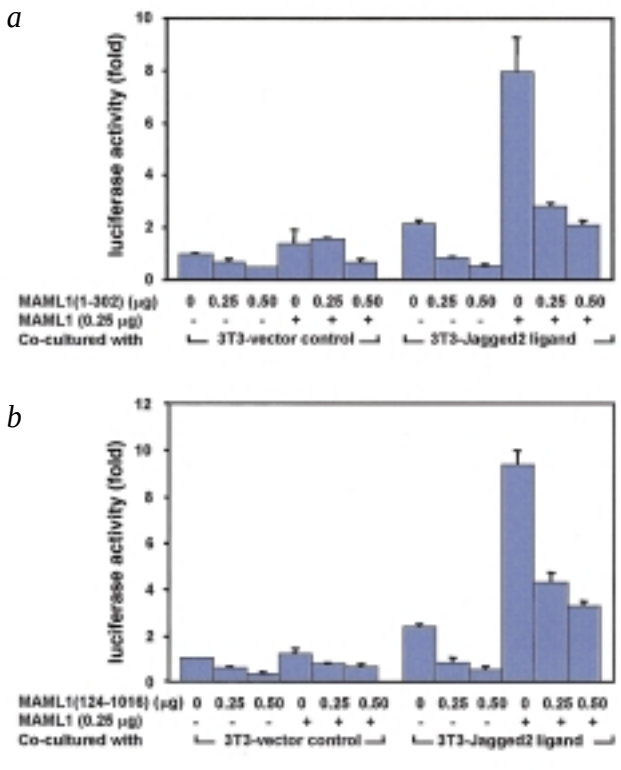

Fig. 6 MAML1 mutants lacking the NOTCH-binding site or the transcriptional activation domain block ligand-induced signalling. U20S cells were transfected with HES1-luc (0.5 μg) and TK-*Renilla* luciferase control reporter construct (0.5 μg), together with increasing amounts of the construct encoding MAML1(1–302) (***a***) or MAML1(124–1016) (***b***) in the absence or the presence of 0.25 μg of the plasmid encoding MAML1. Twenty hours after transfection, 1×10^5 NIH3T3 cells expressing Jagged2 ligands or infected with empty pBABE virus were added to each well. *HES1* reporter luciferase activity, corrected for TK-*Renilla* luciferase activity, is expressed as fold activation relative to cells not expressing MAML1 that were cocultured with control NIH 3T3 cells.

(w/v), NaF (100 M), 1 mM phenylmethylsulphonyl fluoride (PMSF), aprotinin (20 μg/ml), sodium orthovanadate (1 mM; Na_3VO_4) and leupeptin (40 μg/ml). After incubation on ice for 30 min, cell lysates were centrifuged at 12,000*g* for 15 min at 4 °C. To prepare immunoprecipitates, we incubated cell lysates with anti-Flag monoclonal antibody (M2) and anti-mouse IgG agarose (Sigma) for 4 h or overnight at 4 °C. We then washed the agarose beads five times with lysis buffer, and solubilized adsorbed proteins by incubation for 5 min in SDS–PAGE loading buffer at 100 °C. After SDS–PAGE, we eletrophoretically transferred proteins to Protran nitrocellulose membrane (Schleicher and Schuell). Membranes were blocked with 5% non-fat dry milk in TBST (10 mM Tris-HCl, pH 8.0, 150 mM NaCl, 0.05% Tween20) and incubated with primary antibodies overnight at 4 °C. After washing 5 times for 10 min each in TBST, membranes were incubated with HRP-coupled secondary antibodies for 1 h, washed again and stained using a chemiluminescent method (ECL, Amersham).

GST pull-down assay. Polypeptides were synthesized *in vitro* in the presence of [^{35}S] methionine using the TNT coupled reticulocyte lysate system (Promega), and then incubated with GST-fusion proteins or GST bound to glutathione-Sepharose beads (Pharmacia Biotech) for 2 h at 4 °C in NETN (20 mM Tris, pH 7.5, 100 mM NaCl, 5 mM EDTA, 0.5% NP-40). Beads were washed 5 times in NETN and then heated to 100 °C in SDS–PAGE loading buffer for 10 min. ^{35}S-labelled proteins were detected by SDS–PAGE followed by fluorography.

Protein purification. We cloned cDNAs encoding the ANK domain alone (aa 1,872–2,126), or both the RAM and ANK domains (RAM-ANK, aa 1,760–2,126, with an additional hexahistidine tag at the C terminus to facilitate purification) of human NOTCH1 into the prokaryotic expression plasmid pET41-1. To purify ANK, we incubated GST–ANK from BL21(DE3) cell lysates with glutathione-Sepharose beads (Pharmacia). Following release by thrombin cleavage, ANK was purified by anion exchange chromatography on Mono-Q resin (Pharmacia) followed by gel filtration on a Superdex 200 column (Pharmacia). We purified RAM-ANK in an identical fashion, except that it was bound and eluted with an imidazole gradient from Ni-NTA agarose beads (Qiagen) before the Mono-Q chromatography step. A cDNA encoding the N-terminal portion of MAML1(1–300) was cloned into a plasmid derived from pRSET (Invitrogen) that permits expression of polypeptides with a hexahistidine N-terminal tag. MAML1(1–300) was purified from BL21(DE3) cell lysates in a single step by Ni-NTA agarose chromatography using an imidazole gradient. We immunoprecipitated Myc-epitope–tagged RBP-Jκ from 293T cells transfected with a pcDNA3 expression plasmid, using monoclonal anti-Myc antibody 9E10 on protein A-Sepharose beads[27], and eluted the immunoprecipitated RBP-Jκ-Myc by incubation for 60 min at 4 °C in Tris (10 mM, pH 8.0) containing EDTA (1 mM), BSA (0.2 mg/ml), 10% glycerol and Myc epitope peptide (1 mg/ml; Research Genetics). All purified proteins were snap-frozen in liquid nitrogen and stored at –80 °C until use.

EMSA. We incubated ^{32}P-labelled oligonucleotides (10^4 cpm) containing a normal or mutated RBP-Jκ–binding site[28] for 30 min at 30 °C in a 15 μl volume containing Hepes (20 mM, pH 7.9), KCl (60 mM), $MgCl_2$ (5 mM), DTT (10 mM), BSA (0.2 mg/ml), dGdC (250 ng), 10% glycerol in the presence or absence (+ or –) of the following components: 1 μl immunopurified RBP-Jκ, 50 ng RAM-ANK, 50 ng ANK and 50 ng MAML1(1–300). We electrophoresed samples at 140 V in 4% Tris-glycine-EDTA gels, and then dried and analysed the gels by autoradiography.

Reporter assay. We seeded U20S cells on six-well plates at 1×10^5 cells per well 1 d before transfection, and transiently transfected cells with various combinations of expression plasmid DNA (indicated in each figure legend). The total amounts of plasmids were kept constant by adding appropriate amounts of empty vectors without inserts. We collected transfected cells 44 h post-transfection and measured luciferase activities in a Berthold luminometer (Lumat LB9507). Relative luciferase activities were normalized to β-galactosidase activity (in the case of pCMX-lacZ) or *Renilla* luciferase activity (in the case of pRL-TK). We measured β-galactosidase activity using a β-gal assay kit (Invitrogen), and luciferase activities using either single or dual luciferase reporter assay systems (Promega).

GenBank accession number. *MAML1* cDNA sequence, AF221759; *Drosophila mastermind*, X54251; KIAA0200, D83785.

Acknowledgements

We thank K. Kobayashi and V. Patriubavicius for technical assistance, and B. Bernstein and Y. Nam for design and purification of the ANK and RAM-ANK fragments of NOTCH1. Supported by NIH grants CA09362 (L.W.), CA82308 (J.CA.), HL-61001 (S.C.B.), and CA36167, CA66996 and DK50654 (J.D.G.); and Barr-Weaver Funds from Dana-Farber Cancer Institute. S.C.B. is a Pew Scholar in the Biomedical Sciences. S.A.-T is supported by the Howard Hughes Medical Institute

Received 12 June; accepted 2 November 2000.

1. Artavanis-Tsakonas, S., Rand, M.D. & Lake, R.J. Notch signaling: cell fate control and signal integration in development. *Science* **284**, 770–776 (1999).
2. Kopan, R., Schroeter, E.H., Weintraub, H. & Nye, J.S. Signal transduction by activated mNotch: importance of proteolytic processing and its regulation by the extracellular domain. *Proc. Natl Acad. Sci. USA* **93**, 1683–1688 (1996).
3. Tamura, K. *et al.* Physical interaction between a novel domain of the receptor Notch and the transcription factor RBP-J κ/Su(H). *Curr. Biol.* **5**, 1416–1423 (1995).
4. Jarriault, S. *et al.* Signalling downstream of activated mammalian Notch. *Nature* **377**, 355–358 (1995).
5. Smoller, D. *et al.* The Drosophila neurogenic locus mastermind encodes a nuclear protein unusually rich in amino acid homopolymers. *Genes Dev.* **4**, 1688–1700 (1990).
6. Bettler, D., Pearson, S. & Yedvobnick, B. The nuclear protein encoded by the Drosophila neurogenic gene mastermind is widely expressed and associates with specific chromosomal regions. *Genetics* **143**, 859–875 (1996).
7. Yedvobnick, B., Smoller, D., Young, P. & Mills, D. Molecular analysis of the neurogenic locus mastermind of Drosophila melanogaster. *Genetics* **118**, 483–497 (1988).
8. Lehmann, R.F., Jimenez, W., Dietrich, U. & Campos-Ortega, J.A. On the phenotype and development of mutants of early neurogenesis in D. melanogaster. *Wilhelm Roux's Arch. Dev. Biol.* **192**, 62–74 (1983).
9. Aster, J. *et al.* Functional analysis of the TAN-1 gene, a human homolog of Drosophila notch. *Cold Spring Harb. Symp. Quant. Biol.* **59**, 125–136 (1994).
10. Roehl, H., Bosenberg, M., Blelloch, R. & Kimble, J. Roles of the RAM and ANK domains in signaling by the C. elegans GLP-1 receptor. *EMBO J.* **15**, 7002–7012 (1996).
11. Rebay, I., Fortini, M.E. & Artavanis-Tsakonas, S. Analysis of phenotypic abnormalities and cell fate changes caused by dominant activated and dominant negative forms of the Notch receptor in Drosophila development. *C. R. Acad. Sci. III* **316**, 1097–1123 (1993).
12. Helms, W. *et al.* Engineered truncations in the Drosophila mastermind protein disrupt Notch pathway function. *Dev. Biol.* **215**, 358–374 (1999).
13. Hsieh, J.J., Zhou, S., Chen, L., Young, D.B. & Hayward, S.D. CIR, a corepressor linking the DNA binding factor CBF1 to the histone deacetylase complex. *Proc. Natl Acad. Sci. USA* **96**, 23–28 (1999).
14. Kao, H.Y. *et al.* A histone deacetylase corepressor complex regulates the Notch signal transduction pathway. *Genes Dev.* **12**, 2269–2277 (1998).
15. Taniguchi, Y., Furukawa, T., Tun, T., Han, H. & Honjo, T. LIM protein KyoT2 negatively regulates transcription by association with the RBP-J DNA-binding protein. *Mol. Cell. Biol.* **18**, 644–654 (1998).
16. Zhou, S. *et al.* SKIP, a CBF1-associated protein, interacts with the ankyrin repeat domain of NotchIC to facilitate NotchIC function. *Mol. Cell. Biol.* **20**, 2400–2410 (2000).
17. Matsuno, K., Diederich, R.J., Go, M.J., Blaumueller, C.M. & Artavanis-Tsakonas, S. Deltex acts as a positive regulator of Notch signaling through interactions with the Notch ankyrin repeats. *Development* **121**, 2633–2644 (1995).
18. Matsuno, K. *et al.* Human deltex is a conserved regulator of Notch signalling. *Nature Genet.* **19**, 74–78 (1998).
19. Petcherski, A. & Kimble, J. LAG-3 is a putative trancriptional activator in the C. elegans Notch pathway. *Nature* **405**, 364–368 (2000).
20. LaMorte, V.J., Dyck, J.A., Ochs, R.L. & Evans, R.M. Localization of nascent RNA and CREB binding protein with the PML-containing nuclear body. *Proc. Natl Acad. Sci. USA* **95**, 4991–4996 (1998).
21. Doucas, V., Tini, M., Egan, D.A. & Evans, R.M. Modulation of CREB binding protein function by the promyelocytic (PML) oncoprotein suggests a role for nuclear bodies in hormone signaling. *Proc. Natl Acad. Sci. USA* **96**, 2627–2632 (1999).
22. Xu, T., Rebay, I., Fleming, R.J., Scottgale, T.N. & Artavanis-Tsakonas, S. The Notch locus and the genetic circuitry involved in early Drosophila neurogenesis. *Genes Dev.* **4**, 464–475 (1990).
23. Go, M.J. & Artavanis-Tsakonas, S. A genetic screen for novel components of the notch signaling pathway during Drosophila bristle development. *Genetics* **150**, 211–220 (1998).
24. Pear, W.S. *et al.* Efficient and rapid induction of a chronic myelogenous leukemia-like myeloproliferative disease in mice receiving P210 bcr/abl-transduced bone marrow. *Blood* **92**, 3780–3792 (1998).
25. Hawley, R.G., Lieu, F.H., Fong, A.Z. & Hawley, T.S. Versatile retroviral vectors for potential use in gene therapy. *Gene Ther.* **1**, 136–138 (1994).
26. Pui, J.C. *et al.* Notch1 expression in early lymphopoiesis influences B versus T lineage determination. *Immunity* **11**, 299–308 (1999).
27. Aster, J.C. *et al.* Oncogenic forms of NOTCH1 lacking either the primary binding site for RBP-Jκ or nuclear localization sequences retain the ability to associate with RBP-Jκ and activate transcription. *J. Biol. Chem.* **272**, 11336–11343 (1997).
28. Henkel, T., Ling, P.D., Hayward, S.D. & Peterson, M.G. Mediation of Epstein-Barr virus EBNA2 transactivation by recombination signal-binding protein Jκ. *Science* **265**, 92–95 (1994).